Lexicographic multi-objective optimization of thermoacoustic refrigerator's stack

L. K. Tartibu, B. Sun & M. A. E. Kaunda

Heat and Mass Transfer
Wärme- und Stoffübertragung

ISSN 0947-7411
Volume 51
Number 5

Heat Mass Transfer (2015) 51:649-660
DOI 10.1007/s00231-014-1440-z

Springer

Heat Mass Transfer (2015) 51:649–660
DOI 10.1007/s00231-014-1440-z

ORIGINAL

Lexicographic multi-objective optimization of thermoacoustic refrigerator's stack

L. K. Tartibu · B. Sun · M. A. E. Kaunda

Received: 1 November 2013 / Accepted: 25 September 2014 / Published online: 2 October 2014

Abstract This work develops a novel mathematical programming model to optimize the performance of a simple thermoacoustic refrigerator (TAR). This study aims to optimize the geometric parameters namely the stack position, the stack length, the blockage ratio and the plate spacing involved in designing TARs. System parameters and constraints that capture the underlying thermoacoustic dynamics have been used to define the models. The cooling load, the coefficient of performance and the acoustic power loss have been used to measure the performance of the device. The optimization task is formulated as a three-criterion nonlinear programming problem with discontinuous derivatives (DNLP). Since we optimize multiple objectives simultaneously, each objective component has been given a weighting factor to provide appropriate user-defined emphasis. A practical example is given to illustrate the approach. We have determined a design statement of a stack describing how the geometrical parameters describing would change if emphasis is given to one objective in particular. We also considered optimization of multiple objectives components simultaneously and identify global optimal solutions describing the stack geometry using a lexicographic multi-objective optimization scheme. Additionally, this approach illustrates the difference between a design for maximum cooling and best coefficient of performance of a simple TAR.

L. K. Tartibu (✉)
Department of Mechanical Engineering, Mangosuthu University of Technology, Box 12363, Durban 4026, South Africa
e-mail: lagougetartibu@yahoo.fr

B. Sun · M. A. E. Kaunda
Department of Mechanical Engineering, Cape Peninsula University of Technology, Box 652, Cape Town 8000, South Africa

List of symbols

a	Speed of sound (m/s)
BR	Blockage ratio
c_p	Isobaric specific heat capacity (J/kgK)
COP	Coefficient of performance of refrigerator
COPC	Carnot coefficient of performance
COPR	Relative coefficient of performance
dir_i	Direction of ith objective
DR	Drive ratio
f	Frequency (Hz)
K	Thermal conductivity (W/m K)
l	Plate half thickness (mm)
L_S	Stack length (mm)
L_{Sn}	Normalised stack length
min	Minimize
max	Maximize
p_m	Mean pressure (Pa)
r_i	Range of ith objective function
s_i	Surplus of ith objective
T_m	Mean temperature
T_{mn}	Normalized temperature difference
X_S	Stack centre position (mm)
X_{Sn}	Normalised stack position
w_i	Objective function component weight
$\overset{o}{W}_2$	Acoustic power loss
y_o	Plate half-gap (mm)

Greek symbols

δ_k	Gas thermal penetration depth (mm)
δ_{kn}	Normalised thermal penetration depth
δ_s	Solid thermal penetration depth (mm)
δ_v	Viscous penetration depth
γ	Isentropic coefficient
ε_s	Stack heat capacity correction factor

ω	Angular frequency (rad/s)
ρ_m	Density (kg/m^3)
σ	Prandtl number
θ	Normalised temperature difference
ΔT_m	Temperature span (K)
Φ_c	Normalized cooling load
Φ_H	Normalized heat flow
Φ_W	Normalized acoustic power
ξ	Objective function
μ	Dynamic viscosity (kg/m s)
λ	Wavelength (mm)
ε_i	Right hand side of ith objective function

1 Introduction

Thermoacoustic refrigerators (TARs) offer a solution to the current search for alternative refrigerants and alternative technologies (such as absorption refrigeration, thermoelectric refrigeration, pulse-tube refrigeration etc.) to reduce environmental impact [1]. Thermoacoustics is a field of study that combines both acoustic waves and thermodynamics. The interaction of the temperature oscillation accompanied by the pressure oscillation in a sound wave with solid boundaries initiates the energy conversion processes. In ordinary experience, this interaction between heat and sound cannot be observed. It can be amplified under suitable conditions to give rise to significant thermodynamic effects such as convective heat fluxes, steep thermal gradients and strong sound fields. TARs use acoustic power to cause heat flow from low temperature source to high temperature sink. In contrast, thermoacoustic engines (TAEs) produce acoustic power using heat flow from high temperature source to low temperature sink [2].

Thermoacoustic refrigerators (Fig. 1) mainly consist of a loudspeaker (a vibrating diaphragm or thermoacoustic prime mover) attached to a resonator filled with gas, a stack usually made of thin parallel plates and two heat exchangers placed at either side of the stack. The stack forms the heart of the refrigerator where the heat-pumping process takes place, and it is thus an important element which determines the performance of the refrigerator [3]. For the temperature gradient along the stack walls to remain steady, the material selected should have higher heat capacity and lower thermal conductivity than the gas otherwise the stack won't be affected by the temperature oscillations of the nearby gas. In addition, a material of low thermal conductivity should be chosen for the stack and the resonator to prevent leaking from the hot side of the resonator back to the cold side and to withstand higher pressure [4].

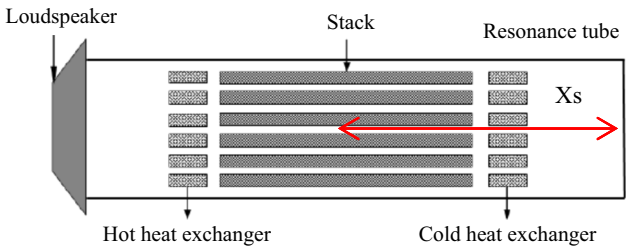

Fig. 1 Schematic diagram of a typical thermoacoustic refrigerator

Using a sound source such as a loudspeaker, an acoustic wave is generated to make the gas resonant. As the gas oscillates back and forth within the chamber, the standing sound wave creates a temperature difference along the length of the stack. This temperature change is a result of compression and expansion of gas by sound pressure and thermal interaction between the oscillating gas and the surface of the plate. Heat is exchanged with the surrounding through heat exchangers at the cold and hot side of the stack [2]. The basic mechanics behind thermoacoustics are already well understood. A detailed explanation of the way thermoacoustic coolers work is given by Swift [3] and Wheatly et al. [5]. Recent researches focuses on improving the performance of the devices so that thermoacoustic coolers can compete with commercial refrigerators. One way to improve the performance of currents devices is through developing novel modelling approach in order to understand interaction between design parameters. After briefly describing the design optimization with regards to TARs and review previous optimization efforts underlying thermoacoustic devices, we will then proceed to discuss our approach to optimize their design.

2 Optimization of thermoacoustic refrigerators

In mathematical sense, optimization is the selection of a best element (with regard to some criteria) from some set of available alternatives. It involves maximizing or minimizing a function of one or more variables. Engineering optimization is the subject which uses optimization techniques to achieve design goals. It can be defined as the process of finding the conditions that give the maximum or minimum value of a function [6]. The optimization criterion can therefore be formulated in mathematical form, as a function (objective function). This study deals with the application of mathematical programming techniques suitable for the solution of engineering design problems.

In the case of TARs, we have used relevant physical parameters describing the device and which determine the performance of the thermoacoustic system form in the optimization process.

For optimization purposes, the thermodynamic analysis of Wetzel and Herman [7] shows that TAR can be subdivided into four modules: (1) thermoacoustic stack, (2) resonance tube, (3) heat exchangers and (4) acoustic driver. Therefore, the designer can optimize each module separately and obtain a maximum global thermodynamic performance of the device as a result. The most important part of the thermoacoustic system is the core, where the stack of plates is [3]. Thermoacoustic effects actually occur within a very small layer next to the plate, the thermal boundary layer. It is defined as [8]:

$$\delta_k = \sqrt{\frac{2K}{\rho_m c_p \omega}} \quad (1)$$

With K being the thermal conductivity, ρ_m the mean density, c_p the constant pressure specific heat capacity of the working fluid. Heat transfer by conduction is encouraged by a thick boundary layer during a period of $1/\omega$, where ω is the angular frequency of the vibrating fluid. However, another layer that occurs next to the plate, the viscous boundary layer, discourages the thermoacoustic effects. It is defined as [8]:

$$\delta_V = \sqrt{\frac{2\mu}{\rho_m \omega}} \quad (2)$$

where μ is the diffusivity of the gas. Losses due to viscous effects occur in this region. A thinner viscous boundary layer than the thermal boundary layer is desirable for effective thermoacoustic effects.

Various parameters affecting the performance of TARs are well understood from previous studies. A network model to evaluate the temperature differences across the stack was developed by Tu et al. [9]. The results found show that the stack position, the oscillating pressure ratios and the stack geometries affect the temperature differences. The optimization of inertance sections of thermoacoustic devices using DeltaEC (Design Environment for low-amplitude Thermoacoustic Energy Conversion) by varying individual parameters to determine optimal designs is illustrated by Zoontjens et al. [10]. Their results highlight a vast array of variables that must be considered interdependent for robust device operation. The performance of a standing wave thermoacoustic cooler to achieve the best possible COPRs (coefficient of performance compared to Carnot) for various temperature spans between the hot and cold side of the stack was evaluated by Paek et al. [11] using DeltaEC. The results found show that thermoacoustic cooling seems to make less sense for applications with either low or high temperature spans such as air conditioning or cryogenic cooling. The impact of the gas blockage with small and large thermal contact areas between stack and heat exchanges on the performance of a TAR was investigated by Akhavanbazaz et al. [12]. The results found shows that increasing the thermal contact area of heat exchangers reduces the cooling load and increases the acoustic power required due to the gas blockage. The performance of a thermoacoustic refrigeration system with respect to temperature difference, the pressure and the frequency was investigated by Nsofor et al. [13]. The results found shows that there is an optimum pressure and an optimum frequency for which the system should be operated in order to obtain maximum cooling load. The relationship between cooling load and plate spacing was derived by Wu et al. [14] using constructural principle. The results found shows that the plate spacing and the number of plate influence the cooling load. A two dimensional numerical simulation of a TAR driven at large amplitude was conducted by Ke et al. [15]. Optimized parameters of plate thickness, length and plate spacing of heat exchangers have been identified. The effect of operation conditions and geometrical parameters on heat exchangers performance in TAR was investigated by Piccolo [16]. Relevant guidance have been drawn for heat exchanger design as far as fin length, fin spacing, blockage ratio, gas and secondary fluid-side heat transfer coefficients are concerned. More recently, Hariharan et al. [17] optimize the parameters like frequency, stack position, stack length, and plate spacing involving in designing TAR using the response surface methodology (RSM). Their results show that geometrical variables chosen for their investigation are interdependent. This is by no means a complete list of the "optimization" of refrigerators components, but it is a good overview of optimization Targets.

3 Motivation

Considering a simple TAR, comprised of a stack inside of a resonance tube, the energy flows are obvious. Acoustic work, sound, can be used to generate temperature differences that allow heat to move from a low temperature reservoir to an ambient at higher temperature, thus forming a thermoacoustic refrigeration system. Therefore, the goal of the optimization is to achieve the highest performance for a particular configuration and set of operating conditions. Interestingly, Herman and Travnicek [18] found that sets of parameters leading to two seemingly similar outcomes, maximum efficiency and maximum cooling were not the same. Therefore, they have considered two optimization criteria in the design optimization of TARs. For a particular set of operating conditions and system configuration, one goal is to achieve the highest COP. This criteria is useful when designing large thermoacoustic system or comparing the performance of refrigeration system. For small-scale thermoacoustic systems, the cooling load was

found to be critical for the success of the design [18]. This work is undoubtedly a valuable addition to the thermoacoustic community. However, this optimization effort relies heavily on studying the effect of a single design parameter on device performance. In all likelihood, each optimal design is a local optimum as the solution obtained is optimal (either maximal or minimal) within a neighbouring set of candidate solution. This is in contrast with the global optimum proposed in this study, which gives global optimal solution among all possible solutions in a specific domain, not just those in particular neighbourhood of variables. We discuss a novel mathematical programming approach to handling design and choice between maximum cooling and maximum coefficient of performance of TAR. Additionally, we have identified the blockage ratio, the stack spacing, the stack length and the position of the stack as design parameters and take their interdependency into account while computing the optimal set describing optimal performance of TARs unlike previous studies.

The remainder of this paper is organized in the following fashion: in Sect. 4, the model development is presented. The fundamental parameters and equations in our mathematical models characterizing the standing wave TARs are presented. In Sect. 5, we discuss single objective optimization, using weighted sum method to find values of the variables that satisfy the constraints and are globally optimal with respect to the considered objective function. Section 6 considers optimization of multiple objectives using a lexicographic optimization scheme. Sections 7 and 8 report the contributions of this work.

4 Model development

In this section, the model development for the physical standing wave refrigerator depicted in Fig. 1 is presented. For our models, only the stack geometry is considered. The model does not consider any effect of the working fluid (details available in Ref. [18]), the stack material or the interdependency of coefficient of performance of thermoacoustic core, effectiveness of heat exchangers and acoustic power efficiency. The geometry used to derive and discuss the thermoacoustic equations is illustrated in Fig. 2. In this paper, no attempt is made to derive these equations, as detailed derivations of the equations are available in both Mahmud [19] and Tijani [20] thesis.

The main assumptions made in the derivation of the heat and the work flows from the exact equation are:

- The short stack approximations and
- the boundary layer approximation

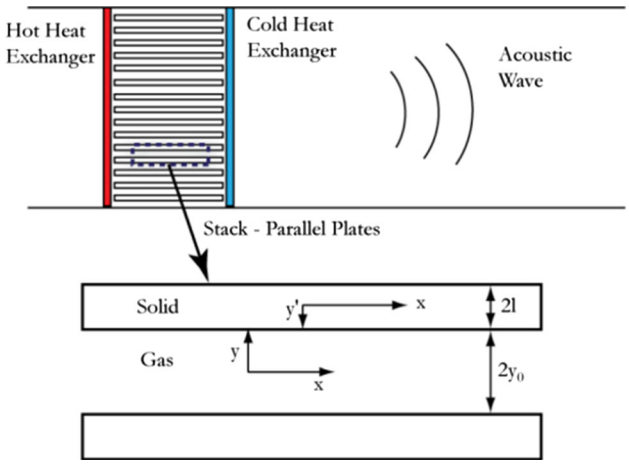

Fig. 2 A simple short stack thermoacoustic engine with stack spacing and thickness

The short stack approximation considered that the stack is short enough ($L_s \ll \lambda$) so that the velocity and the pressure do not vary significantly. The boundary layer approximation considers the plate half thickness and plate half-gap large enough compared to the gas and the solid thermal penetration depth ($y_o \gg \delta_k$ and $1 \gg \delta_s$). This approximation simplifies the coupled equations governing the fluid motion and heat transfer. In addition, under theses approximations, the temperature difference ΔT_m is much less than the mean temperature span T_m. Therefore the thermophysical properties of the stack and the working fluid can be taken as constant. With these assumptions, Tijani et al. [19] have derived acoustic power and heat flow in thermoacoustic element.

4.1 Design parameters of the thermoacoustic core

The basic design requirements for TAR are twofold [18]:

a. To supply the desired cooling load and
b. to achieve the prescribed cooling temperature at the same time

The coefficient of performance of a thermoacoustic core COP is dependent of 19 independent design parameters [7]. Wetzel and Herman [18] have collapsed the number of parameters to the following six normalized parameter spaces.

4.2 Objectives functions

The performance of the thermoacoustic stack depends on three main stack design parameters: the centre position, the length and the cross-section area of the stack. The normalized heat flow Φ_H and acoustic power, Φ_W neglecting

axial conduction in the working fluid as well as in the stack plates, are given by [21]:

$$\Phi_H = -\left[\frac{\delta_{kn} DR^2 \sin(2X_{Sn})}{8\gamma(1+\sigma)\left(1-\sqrt{\sigma}\delta_{kn}+\frac{1}{2}\sigma\delta_{kn}^2\right)}\right] \times \left[\frac{\Delta T_{mn}\tan(X_{Sn})}{(\gamma-1)BR\, L_{Sn}} \times \frac{(1+\sqrt{\sigma}+\sigma)}{1+\sqrt{\sigma}} - \left(1+\sqrt{\sigma}-\sqrt{\sigma}\delta_{kn}\right)\right] \quad (3)$$

$$\Phi_W = \left[\frac{\delta_{kn} DR^2 L_{Sn}(\gamma-1)BR\cos^2(X_{Sn})}{4\gamma}\right] \times \left[\frac{\Delta T_{mn}\tan(X_{Sn})}{BR\, L_{Sn}(\gamma-1)(1+\sqrt{\sigma})\left(1-\sqrt{\sigma}\delta_{kn}+\frac{1}{2}\sigma\delta_{kn}^2\right)} - 1\right] - \left[\frac{\delta_{kn} L_{Sn} DR^2}{4\gamma} \times \frac{\sqrt{\sigma}\sin^2(X_{Sn})}{BR\left(1-\sqrt{\sigma}\delta_{kn}+\frac{1}{2}\sigma\delta_{kn}^2\right)}\right] \quad (4)$$

We can now define the normalized cooling load Φ_C and the coefficient of performance of the thermoacoustic core COP respectively by [7]:

$$\Phi_C = \Phi_H - \Phi_W \quad (5)$$

$$COP = \frac{\Phi_H - \Phi_W}{\Phi_W} \quad (6)$$

The cooling load Φ_C is function of 8 non dimensional parameters [8]:

$$\Phi_C = F(\sigma,\ \gamma,\ \varepsilon_S,\ \theta,\ L_{Sn},\ X_{Sn},\ BR,\ \delta_{kn}) \quad (7)$$

Where σ, γ, ε_S and θ represent respectively the Prandtl number, the polytropic coefficient, the stack heat capacity correction factor and the normalized temperature difference. The influence of the working fluid on the gas is exerted through the parameters σ, γ, and ε_S. In Sects. 5 and 6, we will study the influence of normalized stack length L_{Sn}, normalized stack position X_{Sn}, blockage ratio BR and normalized thermal penetration depth δ_{kn} (as described in Table 1) on the performance of the TAR.

Performance inefficiencies in a TAR arise from heat transfer problems and viscous losses within a viscous penetration depth δ_v, from stack plates and from resonator walls [22]. Stack resistance to sound wave causes intensity attenuation and introduces nonlinearities [23]. Therefore, the viscous and thermal relaxation dissipation in the penetration depth and along the surface of the resonator have to be considered. In the boundary layer approximation, the acoustic power loss per unit area of the resonator is given by [21]:

$$\overset{o}{W}_2 = \frac{dW_2}{dS} = \left[\frac{\delta_{kn} DR^2 L_{Sn}(\gamma-1)BR\ \cos^2(X_{Sn})}{4\gamma}\right] + \left[\frac{\delta_{kn} L_{Sn} DR^2}{4\gamma} \times \frac{\sqrt{\sigma}\sin^2(X_{Sn})}{BR\left(1-\sqrt{\sigma}\delta_{kn}+\frac{1}{2}\sigma\delta_{kn}^2\right)}\right] \quad (8)$$

where the first term on the right-hand side is the kinetic energy dissipated by viscous shear. The second term is the energy dissipated by thermal relaxation.

5 Single objective optimization

All the expressions involved in our mathematical programming model (MPF) have been presented in the previous section. Together with the following expressions, they represent a nonlinear programming problem with discontinuous derivatives (DNLP):

$$(MPF)\ \max_{BR,\delta_{kn},L_{Sn},X_{Sn}} \xi = w_1(\Phi_C) + w_2(COP) + w_3\left(-\overset{o}{W}_2\right) \quad (9)$$

This mathematical model characterizes the essential elements of a standing wave TAR. In the following discussion we analyse restricted cases of our objectives, and identify general tendencies of the parameters to influence

Table 1 TAR parameters

Operation parameter	
Drive ratio (DR)	$DR = \frac{p_0}{p_m}$ where p_0 and p_m are respectively the dynamic and mean pressure
Normalized temperature difference	$\theta = \Delta T_{mn} = \frac{\Delta T_m}{T_m}$ where ΔT_m and T_m are respectively the desired temperature span and the mean temperature span
Gas parameter	
Normalized thermal penetration depth	$\delta_{kn} = \frac{\delta_k}{y_0}$ where $2y_0$ is the plate spacing
Stack geometry parameters	
Normalized stack length	$L_{Sn} = \frac{2\pi f}{a} L_S$ where L_S the stack length
Normalized stack position	$X_{Sn} = \frac{2\pi f}{a} X_S$ where f, a and X_s are respectively the resonant frequency, the speed of sound and the stack centre position
Blockage ratio or porosity	$BR = \frac{y_0}{(y_0+l)}$ where 2 l is the plate thickness

Table 2 Design parameters

Design requirements		
Mean pressure	Pm (Pa)	500,000
Drive ratio	DR (%)	3.5
Normalized temperature difference	θ or ΔT_{mn}	0.030
Stack material	Mylar	

Table 3 Additional parameters

Working fluid: helium		
Prandtl number	σ	0.67
Polytropic coefficient	γ	1.63
Calculated parameters		
Sound speed	a (m/s)	1,054.4
Resonant frequency, a/λ	f (Hz)	24,752
Thermal penetration depth	δ_k (mm)	0.023

individual objective components. To illustrate our approach, we consider the design requirement as described in [18]. It consists of a parallel-plate stack placed in helium-filled resonator. All relevant parameters are given in Tables 2 and 3.

5.1 Emphasizing acoustic cooling load

All proposed models DNLP are solved by GAMS 23.8.1 [24], using LINDOGLOBAL solver on a personal computer Pentium IV 2.1 GHz with 4 GB RAM. The following constraints (upper and lower bounds) have been enforced on variables in other for the solver to carry out the seasrch of the optimal solutions in those ranges:

$$\begin{aligned} &L_{Sn}.lo = 0.001; \quad L_{Sn}.up = 0.500; \\ &X_{Sn}.lo = 0.010; \quad X_{Sn}.up = 1.000 \\ &BR.lo = 0.700; \quad BR.up = 0.900; \\ &\delta_{kn}.lo = 2\delta_k; \quad \delta_{kn}.up = 4\delta_k \quad [8] \end{aligned} \tag{10}$$

Setting the objective function weights to $w_2 = w_3 = 0$ and $w_1 = 1$ in Eq. (9), the problem reduces to Eqs. (3)–(5), and variable restrictions (10). Objective function (9) becomes:

$$\max_{BR,\delta_{kn},L_{Sn},X_{Sn}} \xi_{\Phi_C} = (\Phi_C) \tag{11}$$

In our approach, the geometry range is small in order to illustrate the behaviours of the objective

functions and optimal solution of a small-scale TAR. In Table 4, the optimal solutions that maximize $\xi_{\Phi c}$ are represented with letter superscripted with asterisk:

Physically, this optimal solution can be interpreted as:

- making the stack as short as possible $\left(L^*_{Sn} = L_{Sn\ min}\right)$,

Table 4 Optimal solutions found by LINDOGLOBAL

	L^*_{Sn}	X^*_{Sn}	BR^*	δ^*_{kn}	Φ^*_C	CPU time (s)
x^*	0.001	0.010	0.700	0.046	7.2659E − 4	10.383

Table 5 Optimal solutions found by LINDOGLOBAL

	L^*_{Sn}	X^*_{Sn}	BR^*	δ^*_{kn}	COP^*	CPU time (s)
x^*	0.001	0.014	0.700	0.065	32.8	0.206

- moving the stack as near as possible to the loudspeaker $\left(X^*_{Sn} = X_{Sn\ min}\right)$ and,
- reducing the porosity of the stack $\left(BR^* = BR_{min}\right.$ and $\left.\delta_{kn} = \delta_{kn\ min}\right)$

The maximum cooling load (Table 4)

$$\Phi_{C\ max} = 7.2659E - 4. \tag{12}$$

The decision maker can also determine the minimum cooling load by formulating the problem as follow:

Setting the objective function weights to $w_2 = w_3 = 0$ and $w_1 = 1$in Eq. (9), the problem reduces to Eqs. (3)–(5), and variable restrictions (10). Objective function (9) becomes:

$$\min_{BR,\delta_{kn},L_{Sn},X_{Sn}} \xi_{\Phi_C} = (\Phi_C) \tag{13}$$

The minimum cooling load

$$\Phi_{C\ min} = 4.3339E - 8. \tag{14}$$

$\Phi_{C\ max}$ and $\Phi_{C\ min}$ have been used as upper and lower bounds for the objective Φ_C in the models.

5.2 Emphasizing coefficient of performance

We emphasize COP by setting objective function weights $w_1 = w_3 = 0$ and $w_2 = 1$ in Eq. (9). The problem then simplifies to Eqs. (3), (4), (6), and variable restrictions (10). The maximal performance for all refrigerators is given by the Carnot coefficient of performance obtained as follows [7]:

$$COP_C = \frac{(2-\theta)}{2\theta} \tag{15}$$

This value is used as the upper bound for the objective COP. Objective function (9) becomes:

$$\max_{BR,\delta_{kn},L_{Sn},X_{Sn}} \xi_{COP} = (COP) \tag{16}$$

In Table 5, the optimal solutions that maximize ξ_{COP} are represented with letter superscripted with asterisk.

Physically, this optimal solution can be interpreted as:

- making the stack as short as possible $\left(L^*_{Sn} = L_{Sn\ min}\right)$,
- moving the stack slightly from the loudspeaker $\left(X^*_{Sn} > X_{Sn\ min}\right)$ and,

- reducing the porosity of the stack and making the stack spacing greater then $\delta_{kn\ min}$ $(BR^* = BR_{min}$ and $\delta_{kn} > \delta_{kn\,min})$.

5.3 Emphasizing acoustic power loss

We emphasize $\overset{o}{W}_2$ by setting objective function weights $w_1 = w_2 = 0$ and $w_3 = 1$ in Eq. (9). The problem then simplifies to Eqs. (8) and (9), and variable restrictions (10). The objective function (9) becomes:

$$\max_{BR,\delta_{kn},L_{Sn},X_{Sn}} \xi_{\overset{o}{W}_2} = \left(-\overset{o}{W}_2\right) \tag{17}$$

In Table 6, the optimal solutions that minimize $\xi_{\overset{o}{W}_2}$ are represented with letter superscripted with asterisk.

Physically, this optimal solution can be interpreted as:

- making the stack as short as possible $\left(L^*_{Sn} = L_{Sn\,min}\right)$,
- moving the stack as near as possible to the loudspeaker $\left(X^*_{Sn} = X_{Sn\,min}\right)$ and,
- reducing the porosity of the stack $(BR^* = BR_{min}$ and $\delta_{kn} = \delta_{knmin})$

5.4 Single objective optima: variable analysis

Table 7 summarizes the results of Sects. 5.1, 5.2 and 5.3. It highlights the behaviour of parameters. For these objectives, ↑ indicates an increasing tendency, ↓ indicates a decreasing tendency, and ∓ indicates there is conflicting tension between parameters. Note the lack of tension in parameters for the cooling load Φ_c and the acoustic power loss $\overset{o}{W}_2$, which share the same optimal solution.

Table 6 Optimal solutions found by LINDOGLOBAL

	L^*_{Sn}	X^*_{Sn}	BR^*	δ^*_{kn}	$\overset{o}{W}_2{}^*$	CPU time (s)
x^*	0.001	0.010	0.700	0.046	3.8121E − 9	0.347

Table 7 Tendency of parameters when optimizing individual components

	Φ_c	COP	$\overset{o}{W}_2$
L_{Sn}	↓	↓	↓
X_{Sn}	↓	↑∓	↓
BR	↓	↓	↓
δ_{kn}	↓	↑∓	↓

6 Emphasizing all objective components

Lastly, we simultaneously consider all three objective components by regarding cooling load Φ_c, coefficient of performance COP, and acoustic power lost $\overset{o}{W}_2$ as three distinct objective components. Most of the expressions involved in the formulation of the multi-objective mathematical programming problem (MPF) have been presented in the previous section. The optimization task is formulated as a three-criterion DNLP that simultaneously maximize the magnitude of the cooling load Φ_c, maximize the coefficient of performance COP and minimize acoustic power lost $\overset{o}{W}_2$.

$$(\text{MPF}) \max_{L_{Sn},X_{Sn},BR,\delta_{kn}} \xi = \left\{ \begin{array}{c} \Phi_{C\,(L_{Sn},X_{Sn},BR_a\delta_{kn})}, \\ \text{COP}_{(L_{Sn},X_{Sn},BR_a\delta_{kn})}, \\ -\overset{o}{X}_{2(L_{Sn},X_{Sn},BR_a\delta_{kn})} \end{array} \right\} \tag{18}$$

Subject to bound limits (12), (14) and (15) and the following constraint:

$$\Phi_C = \Phi_H - \Phi_W > 0 \tag{19}$$

A negative cooling load does not have any physical meaning and thus the solutions for which this condition is not met have been eliminated. In the formulation (18), (L_{Sn}, X_{Sn}, BR, δ_{kn}) denotes the parameters of the TAR.

There is no single optimal solution that simultaneously optimizes all the three objectives functions. In these cases, the decision makers are looking for the "most preferred" solution. To find the most preferred solution of this multi-objective model, the augmented ε-constraint method (AUGMECON) as proposed by Mavrotas [25] is applied. The AUGMECON method has been coded in GAMS. The code is available in the GAMS library (http://www.gams.com/modlib/libhtml/epscm.htm) with an example. While the part of the code that has to do with the example (the specific objective functions and constraints), as well as the parameters of AUGMENCON have been modified in this case, the part of the code that performs the calculation of payoff table with lexicographic optimization and the production of the Pareto optimal solutions is fully parameterized in order to be ready to use.

Practically, the ε-constraint method is applied as follows:

- A single primary objective function is maximized while the other are used as constraints.
- From the payoff table the range of each one of the p-1 objective functions that are going to be used as constraints is obtained.
- Then the range of the ith objective function to q_i equal intervals using $(q_i - 1)$ intermediate equidistant grid

points is divided. Thus in total $(q_i + 1)$ grid points that are used to vary parametrically the right hand side (ε_i) of the ith objective function is obtained. The total number of runs becomes $(q_2 + 1) \times (q_3 + 1) \times \ldots \times (q_p + 1)$.

The ε-constraint method has several important advantages over traditional weighted method. These advantages are listed in Ref. [25]. In the conventional ε-constraint method, there is no guarantee that the obtained solutions from the individual optimization of the objective functions are Pareto optima or efficient solutions. In order to overcome this deficiency, the lexicographic optimization for each objective functions to construct the payoff table for the multi-objective mathematical programming models (MPF) is proposed in order to yield only Pareto optimal solutions (it avoids the generation of weakly efficient solutions) [25]. The mathematical details of computing payoff table for the MPF can be found in Ref. [26].

The choice of the primary objective function (most important function) depends on the decision-maker. Often, this decision is based on the problem information and can lead to partial representation of Pareto optimal sets due to tendency of the solution to cluster toward the maximum of the primary objective function. We have therefore articulated the preferences and specify limits on objective functions rather than relying on relative importance of objectives as suggested by Marler [27] to identify the best problem formulation. Subsequently, the augmented ε-constraint method for solving model (Eq. 18) has been formulated twice and most preferred optimal solution have been identified based on the value of the obtained cooling load Φ_C and coefficient of performance COP:

a. Model A

$$\begin{aligned} &\max\left(\Phi_{C\,(L_{Sn},X_{Sn},BR,\delta_{kn})} + dir_1 r_1 \times \left(\frac{s_2}{r_2}+\frac{s_3}{r_3}+\frac{s_4}{r_4}+\frac{s_5}{r_5}\right)\right) \\ &\text{s.t.}\quad COP_{(L_{Sn},X_{Sn},BR,\delta_{kn})} - dir_2 s_2 = \varepsilon_2 \\ &\overset{o}{W}_{2\,(L_{Sn},X_{Sn},BR,\delta_{kn})} - dir_3 s_3 = \varepsilon_3 \\ &s_i \in \Re^+ \end{aligned} \tag{20}$$

b. Model B

$$\begin{aligned} &\max\left(COP_{(L_{Sn},X_{Sn},BR,\delta_{kn})} + dir_1 r_1 \times \left(\frac{s_2}{r_2}+\frac{s_3}{r_3}+\frac{s_4}{r_4}+\frac{s_5}{r_5}\right)\right) \\ &\text{s.t.}\quad \Phi_{C\,(L_{Sn},X_{Sn},BR,\delta_{kn})} - dir_2 s_2 = \varepsilon_2 \\ &\overset{o}{W}_{2(L_{Sn},X_{Sn},BR,\delta_{kn})} - dir_3 s_3 = \varepsilon_3 \\ &s_i \in \Re^+ \end{aligned} \tag{21}$$

where dir_i is the direction of the ith objective function, which is equal to -1 when the ith function should be minimized, and equal to $+1$, when it should be maximized. Efficient solutions of the problem are obtained by parametrical iterative variations in the ε_i. s_i are the introduced surplus variables for the constraints of the MP problem. $r_1 s_i / r_i$ is used in the second term of the objective function, in order to avoid any scaling problem. The formulation of Eqs. (20) and (21) are known as the augmented ε-constraint method due to the augmentation of the objective function Φ_C and COP by the second term. The following constraints (upper and lower bounds) have been enforced on variables in other for the solver to carry out the search of the optimal solutions in those ranges:

$$\begin{aligned} &X_{Sn}.lo = 0.010; \quad X_{Sn}.up = 1.000 \\ &BR.lo = 0.700; \quad BR.up = 0.900; \\ &\delta_{kn}.lo = 2\delta_k; \quad \delta_{kn}.up = 4\delta_k \end{aligned} \tag{22}$$

We use lexicographic optimization for the payoff table; the application of model (Eqs. 20, 21) will provide only the Pareto optimal solutions, avoiding the weakly Pareto optimal solutions. Efficient solutions of the proposed model have been found using AUGMENCON method and the LINDOGLOBAL solver. To save computational time, the early exit from the loops as proposed by Mavrotas [25] has been applied. The range of each five objective functions is divided in four intervals (five grid points). The normalized stack length L_{Sn} has been arbitrarily given successively values of 0.05–0.1–0.15–0.2–0.25–0.3–0.35–0.4–0.5. This process generates optimal solutions corresponding to each value of L_{Sn}. The following section report only the best sets of Pareto solutions obtained successively with model A and B. These results suggest that for an arbitrary chosen fixed value of L_{Sn}, a maximum value of Φ_C and COP can be found. The maximum CPU time taken to complete the results is 324.981 s.

In Figs. 3 and 4 the results of performance calculations illustrating the efficiency of thermoacoustic core, are shown. They are represented in terms of maximum cooling and Coefficient of performance relative to Carnot COPR. Presenting the results in form of COPR instead of COP offers the advantage of not taking into account the trivial part of the Carnot part of the performance, accounting for the temperature dependence of the efficiency. In terms of normalized design parameters, the COPR can be determined as [7]

$$COPR = \frac{COP}{COP_C} = \frac{(|\Phi_H| - |\Phi_W|)/|\Phi_W|}{(2-\theta)/(2\theta)} \tag{23}$$

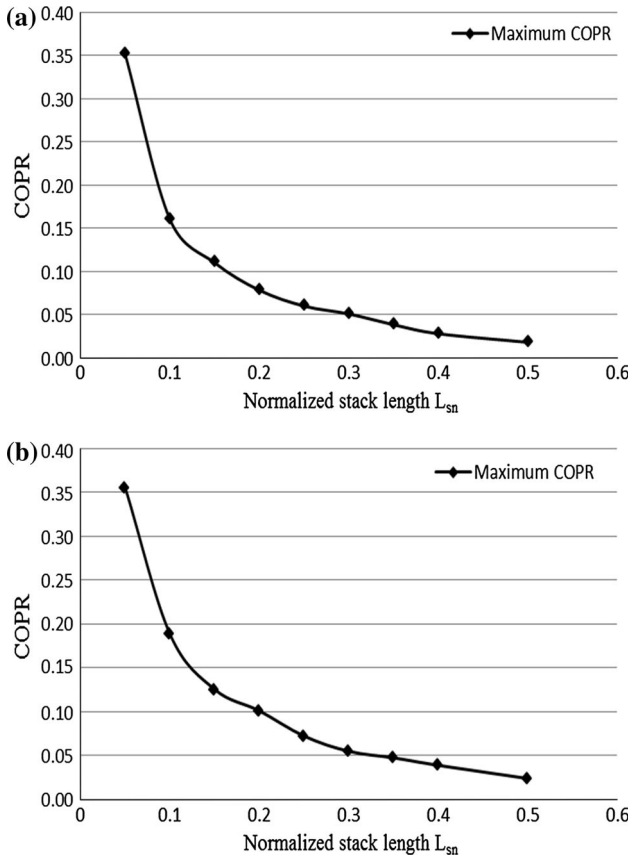

Fig. 3 **a** Cooling load as function of the normalized stack length for model A and **b** Cooling load function of the normalized stack length for model B in Table 8

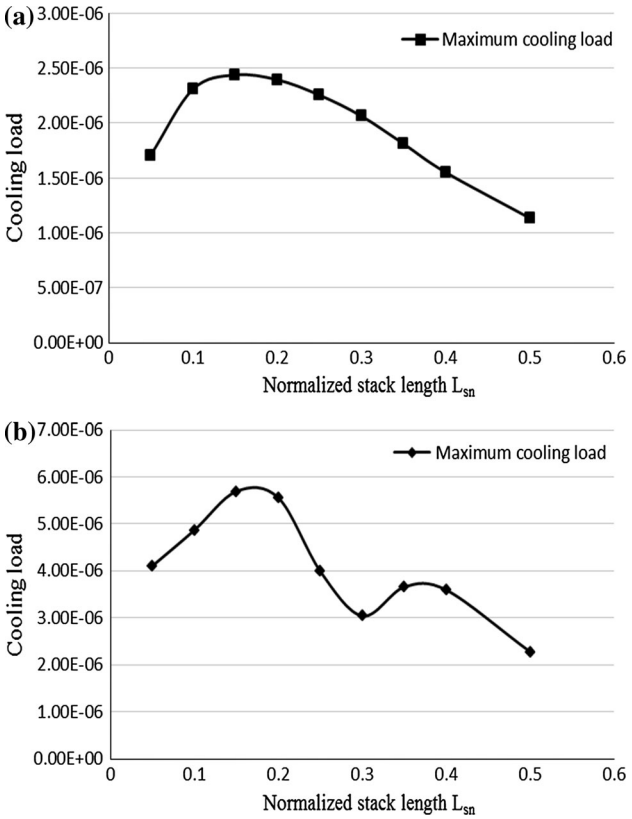

Fig. 4 **a** Coefficient of performance relative to Carnot for model A and **b** Coefficient of performance relative to Carnot for model B in Table 8

7 Results and discussions

7.1 Optimization for best coefficient of performance

In Fig. 3, results that quantify the effect of the normalized stack length on the COPR are displayed. For this purpose, the normalized stack length L_{Sn}, the normalized stack position X_{Sn}, the blockage ratio BR and the normalized thermal penetration depth δ_{kn} were allowed to vary simultaneously and optimal solutions describing the best parameters have been obtained and highlighted in bold in Table 8. The results suggest the COPR increases by locating the stack centre position closer (as compared to the cooling load) to the pressure antinode (closed end) and making the stack length (L_{Sn}) shorter. This concurs with previous studies by Herman and Travnicek [18] who suggest that higher pressure amplitudes at the pressure antinode (closed end) cause more pronounced temperature change.

The results suggest that there is a distinct optimum of the coefficient of performance for a selected set of design parameters and depending on the formulation adopted (model A or B) with the maximum value described by:

Model A

$$\mathrm{COPR}^* = \begin{bmatrix} L_{Sn}^* \\ X_{Sn}^* \\ BR^* \\ \delta_{kn}^* \end{bmatrix} = \begin{bmatrix} 0.050 \\ 0.193 \\ 0.700 \\ 0.046 \end{bmatrix}$$

Model B

$$\mathrm{COPR}^* = \begin{bmatrix} L_{Sn}^* \\ X_{Sn}^* \\ BR^* \\ \delta_{kn}^* \end{bmatrix} = \begin{bmatrix} 0.050 \\ 0.413 \\ 0.720 \\ 0.089 \end{bmatrix}$$

The COPR presented in this study is roughly 35 % of Carnot COP. While considering the losses (viscous and thermal) along the stack, the heat exchangers, the resonator, the heat leaks through the stack and the resonator and the efficiency of a loudspeaker, the COPR of a complete TAR will be lower than the COPR of a stack as presented in this study.

7.2 Optimization for maximum cooling

In this approach, we have taken the interaction between design parameters into account. As shown in Table 8 and

Table 8 Non-dominated solutions found by AUGMENCON

	L_{Sn}	0.050	0.100	0.150	0.200	0.250	0.300	0.35	0.4	0.5
Model A										
COP_{MAX}	BR	**0.700**	0.700	0.700	0.700	0.700	0.700	0.700	0.700	0.700
	δ_{kn}	**0.046**	0.046	0.046	0.046	0.046	0.046	0.046	0.046	0.046
	X_{Sn}	**0.193**	0.426	0.303	0.388	0.321	0.479	0.467	0.454	0.473
	Φ_c	**1.26E−06**	2.31E−06	1.81E−06	2.09E−06	1.59E−06	2.05E−06	1.81E−06	1.55E−06	1.13E−06
	COP	**11.521**	5.250	3.603	2.559	1.958	1.660	1.250	0.910	0.584
$\Phi_{c\ MAX}$	BR	0.700	0.700	**0.700**	0.700	0.700	0.700	0.700	0.700	0.700
	δ_{kn}	0.046	0.046	**0.046**	0.046	0.046	0.046	0.046	0.046	0.046
	X_{Sn}	0.331	0.426	**0.459**	0.478	0.484	0.483	0.467	0.454	0.473
	Φ_c	1.71E−06	2.31E−06	**2.44E−06**	2.39E−06	2.25E−06	2.06E−06	1.81E−06	1.55E−06	1.13E−06
	COP	9.475	5.250	**3.434**	2.432	1.921	1.590	1.250	0.91	0.584
Model B										
COP_{MAX}	BR	**0.720**	0.900	0.835	0.890	0.760	0.860	0.817	0.728	0.808
	δ_{kn}	**0.089**	0.082	0.060	0.460	0.046	0.046	0.046	0.046	0.046
	X_{Sn}	**0.413**	0.521	0.503	0.575	0.610	0.610	0.610	0.517	0.610
	Φ_c	**4.11E−0.6**	4.87E−06	3.74E−06	2.54E−06	2.47E−06	2.33E−06	2.33E−06	2.12E−06	1.31E−06
	COP	**11.65**	6.176	4.109	3.306	2.362	1.795	1.795	1.271	0.778
$\Phi_{c\ MAX}$	BR	0.720	0.900	**0.900**	0.900	0.900	0.900	0.700	0.835	0.700
	δ_{kn}	0.089	0.082	**0.083**	0.084	0.070	0.059	0.078	0.078	0.048
	X_{Sn}	0.413	0.521	**0.561**	0.582	0.656	0.609	0.489	0.628	0.519
	Φ_c	4.11E−06	4.87E−06	**5.70E−06**	5.56E−06	3.99E−06	3.04E−06	3.66E−06	3.59E−06	2.27E−06
	COP	11.65	6.176	**3.429**	2.427	2.118	1.361	1.324	0.928	0.455

Fig. 4, the maximum of the cooling load $\Phi_{C\ MAX}$ is located far away (as compared with best COPR) from the acoustic driver as suggested by values of optimal stack centre position X_{Sn}obtained.

The results suggest that there is a distinct optimum of the cooling load for a selected set of design parameters and depending on the formulation adopted (model A or B) with the maximum value described by:

Model A

$$\Phi_C^* = \begin{bmatrix} L_{Sn}^* \\ X_{Sn}^* \\ BR^* \\ \delta_{kn}^* \end{bmatrix} = \begin{bmatrix} 0.150 \\ 0.459 \\ 0.700 \\ 0.046 \end{bmatrix}$$

Model B

$$\Phi_C^* = \begin{bmatrix} L_{Sn}^* \\ X_{Sn}^* \\ BR^* \\ \delta_{kn}^* \end{bmatrix} = \begin{bmatrix} 0.150 \\ 0.561 \\ 0.900 \\ 0.083 \end{bmatrix}$$

Based on Table 8 and Figs. 3 and 4, one will suspect that the normalized stack length L_{Sn}, the normalized stack position X_{Sn}, the blockage ratio BR and the normalized thermal penetration depth δ_{kn} are somehow related. Indeed, that is the case.

7.3 Best coefficient of performance and maximum cooling load results comparisons

A comparison of Fig. 5a, b leads to the conclusion the maxima of the functions Φ_C^* and $COPR^*$ depends on the mathematical programming formulation. It can be seen that model B (with the COP as primary objective function) produces the highest optimal cooling load Φ_C^* and coefficient of performance $COPR^*$.

This choice is in line with the a priori articulation of preferences by the decision maker which consist of selecting the most preferred solution. Additionally, the maxima of the functions Φ_C^* and $COPR^*$ do not coincide. While the former is far away from the closed end, the latter is close to it. For electronic cooling, the main objective is to achieve high cooling loads; thus, maximising Φ_C^* while maximising the $COPR^*$, is the goal for large-scale devices. Therefore, the solution to this problem exists, given as follow:

Large scale applications:

$$COPR^* = \begin{bmatrix} L_{Sn}^* \\ X_{Sn}^* \\ BR^* \\ \delta_{kn}^* \end{bmatrix} = \begin{bmatrix} 0.050 \\ 0.413 \\ 0.720 \\ 0.089 \end{bmatrix} \text{ or } \begin{bmatrix} 0.050 \\ 0.193 \\ 0.700 \\ 0.046 \end{bmatrix}$$

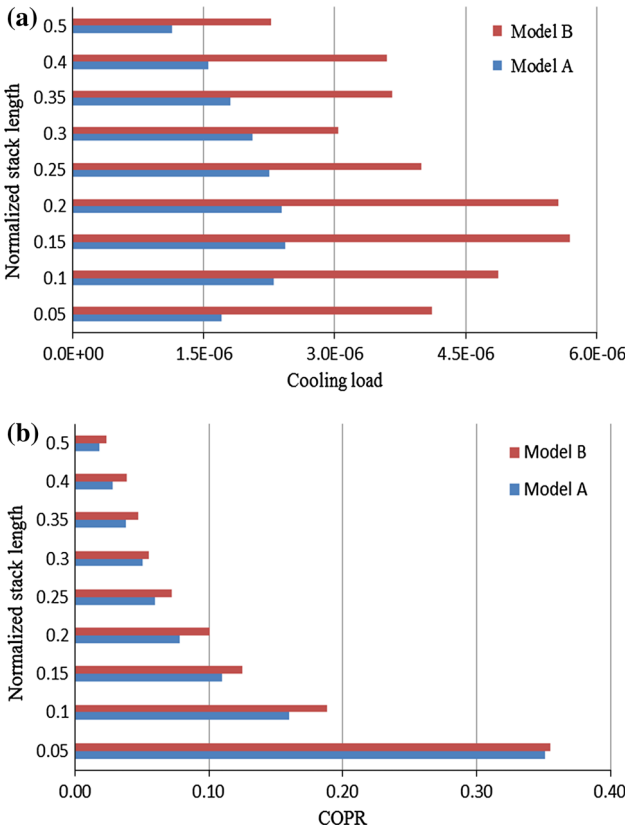

Fig. 5 **a** Results comparison of maximum cooling and **b** best coefficient of performance for model A and B

Electronic cooling applications:

$$\Phi_C^* = \begin{bmatrix} L_{Sn}^* \\ X_{Sn}^* \\ BR^* \\ \delta_{kn}^* \end{bmatrix} = \begin{bmatrix} 0.150 \\ 0.561 \\ 0.900 \\ 0.083 \end{bmatrix} \text{ or } \begin{bmatrix} 0.150 \\ 0.459 \\ 0.700 \\ 0.046 \end{bmatrix}$$

8 Conclusion

In this paper, a multi-objective approach that provides fast initial engineering estimates to initial design calculation of TARs is discussed. Their performances were evaluated using three criteria: (1) maximum cooling, (2) best coefficient of performance, and (3) the acoustic power loss. Four different parameters—stack length, stack centre position, stack spacing and blockage ratio—describing the geometry of the device have been studied. DNLPs have been formulated and implemented in GAMS. For the case of multiple objectives considered simultaneously, we have applied an improved version of a multi-objective solution method, the epsilon-constraint method called augmented epsilon-constraint method (AUGMENCON). We have adopted a lexicographic method in order to avoid dominated Pareto optimal solutions. We were able to identify the best mathematical programming formulation leading to the highest performance of the device. For different arbitrary values of stack length, this process generates optimal solutions describing geometry of the TAR, solutions which depend on the a priori design goal for maximum cooling or maximum coefficient of performance. This present study reveals and quantifies that the results obtained with these two objectives are different. There is a specific stack length which corresponds to a specific stack centre position, specific stack spacing and a specific blockage ratio depending on the design goal. In conclusion, it was determined that the design parameters are interdependent. This clearly supports the use of a lexicographic multi-objective optimisation scheme to design TARs.

References

1. Joshi YK, Garimella SV (2003) Thermal challenges in next generation electronic systems. Microelectron J 34(3):169
2. Swift GW (2002) Thermoacoustics: a unifying perspective for some engines and refrigerators. Acoustical society of America, Melville
3. Swift GW (1988) Thermoacoustic engines. J Acoust Soc Am 4:1146–1180
4. Tijani MEH, Zeegers JCH, De Waele ATAM (2002) Construction and performance of a thermoacoustic refrigerator. Cryogenics 42(1):59–66
5. Wheatley JC, Hofler T, Swift GW, Migliori A (1985) Understanding some simple phenomena in thermoacoustics with applications to acoustical heat engines. Am J Phys 53:147–162
6. Rao SS (1996) Engineering Optimization: theory and practice, 3rd edn. New York, Wiley
7. Wetzel M, Herman C (1997) Design optimization of thermoacoustic refrigerators. Int J Refrig 20(1):3–21
8. Tijani MEH, Zeegers JCH, De Waele ATAM (2002) The optimal stack spacing for thermoacoustic refrigeration. J Acoust Soc Am 112(1):128–133
9. Tu Q, Chen ZJ, Liu JX (2005) Numerical simulation of loudspeaker-driven thermoacoustic refrigerator. Proceedings of the twentieth International Cryogenic Engineering Conference (ICEC 20). Beijing, China
10. Zoontjens L, Howard CQ, Zander AC(2006) Modelling and optimization of acoustic inertance segments for thermoacoustic devices. First Australasian Acoustical Societies 'Conference: Acoustics: Noise of Progress, Clearwater Resort. Christchurch, New Zealand, 435–441
11. Paek I, Braun JE, Mongeau L (2007) Evaluation of standing-wave thermoacoustic cycles for cooling applications. Int J Refrig 30(6):1059–1071
12. Akhavanbazaz M, Kamran Siddiqui MH, Bhat RB (2007) The impact of gas blockage on the performance of a thermoacoustic refrigerator. Exp Thermal Fluid Sci 32(1):231–239
13. Nsofor EC, Ali A (2009) Experimental study on performance of thermoacoustic refrigerating system. Appl Therm Eng 29(13):2672–2679
14. Wu F, Chen L, Shu A (2009) Constructal design of stack filled with parallel plates in standing-wave thermo-acoustic cooler. Cryogenics 49(3–4):107–111
15. Ke H-B, Liu Y-W, He Y-L (2010) Numerical simulation and parameter optimization of thermoacoustic refrigerator driven at large amplitude. Cryogenics 50(1):28–35

16. Piccolo A (2011) Numerical computation for parallel plate thermoacoustic heat exchangers in standing wave oscillatory flow. Int J Heat Mass Transf 54(21–22):4518–4530
17. Hariharan NM, Sivashanmugam P (2013) Optimization of thermoacoustic refrigerator using response surface methodology. J Hydrodyn 25(1):72–82
18. Herman C, Travnicek Z (2006) Cool sound: the future of refrigeration? Thermodynamic and heat transfer issues in thermoacoustic refrigeration. Heat Mass Transfer 42(6):492–500
19. Mahmud S. (2005). MHD and porous media thermoacoustic stacks optimisation, Ph.D. thesis, Department of Mechanical Engineering, University of Waterloo, Waterloo, ON, Canada
20. Tijani MEH (2001) Loudspeaker-driven thermo-acoustic refrigeration, Ph.D. thesis, Eindhoven University of Technology, Netherlands
21. Tijani MEH, Zeegers JCH, De Waele ATAM (2002) Design of thermoacoustic refrigerators. Cryogenics 42(1):49–57
22. Abdel-Rahman E, Azenui NC, Korovyanko I & Symko OG (2002) Size considerations in interfacing thermoacoustic coolers with electronics. Thermomechanical Phenomena in Electronic Systems-Proceedings of the Intersociety Conference. p 421
23. Kuntz HL, Blackstock DT (1987) Attenuation of intense sinusoidal waves in air-saturated, bulk porous materials. J Acoust Soc Am 81(6):1723–1731
24. Generalized Algebraic modelling Systems, (GAMS), [online]. http://www.gams.com
25. Mavrotas G (2009) Effective implementation of the ε-constraint method in multi-objective mathematical programming problems. Ap Math Comp 213:455–465
26. Aghaei J, Amjady N, Shayanfar HA (2009) Multi-objective electricity market clearing considering dynamic security by lexicographic optimization and augmented epsilon constraint method". Appl Soft Comp 11(4):3846–3858
27. Marler T (2009) A Study of multi-objective optimization methods for engineering applications. VDM Verlag, Saarbrucken